Extraordinary-Log Surface Phase Transition in the Three-Dimensional *XY* Model

Minghui Hu,[1] Youjin Deng,[2,3,*] and Jian-Ping Lv[1,†]

[1]*Department of Physics and Anhui Key Laboratory of Optoelectric Materials Science and Technology, Key Laboratory of Functional Molecular Solids, Ministry of Education, Anhui Normal University, Wuhu, Anhui 241000, China*

[2]*Hefei National Laboratory for Physical Sciences at Microscale and Department of Modern Physics, University of Science and Technology of China, Hefei, Anhui 230026, China*

[3]*MinJiang Collaborative Center for Theoretical Physics, College of Physics and Electronic Information Engineering, Minjiang University, Fuzhou 350108, China*

(Received 11 April 2021; revised 23 May 2021; accepted 11 August 2021; published 16 September 2021)

Universality is a pillar of modern critical phenomena. The standard scenario is that the two-point correlation algebraically decreases with the distance r as $g(r) \sim r^{2-d-\eta}$, with d the spatial dimension and η the anomalous dimension. Very recently, a logarithmic universality was proposed to describe the extraordinary surface transition of the $\mathrm{O}(N)$ system. In this logarithmic universality, $g(r)$ decays in a power of logarithmic distance as $g(r) \sim (\ln r)^{-\hat{\eta}}$, dramatically different from the standard scenario. We explore the three-dimensional XY model by Monte Carlo simulations, and provide strong evidence for the emergence of logarithmic universality. Moreover, we propose that the finite-size scaling of $g(r, L)$ has a two-distance behavior: simultaneously containing a large-distance plateau whose height decays logarithmically with L as $g(L) \sim (\ln L)^{-\hat{\eta}'}$ as well as the r-dependent term $g(r) \sim (\ln r)^{-\hat{\eta}}$, with $\hat{\eta}' \approx \hat{\eta} - 1$. The critical exponent $\hat{\eta}'$, characterizing the height of the plateau, obeys the scaling relation $\hat{\eta}' = (N-1)/(2\pi\alpha)$ with the RG parameter α of helicity modulus. Our picture can also explain the recent numerical results of a Heisenberg system. The advances on logarithmic universality significantly expand our understanding of critical universality.

DOI: 10.1103/PhysRevLett.127.120603

Introduction.—Continuous phase transitions are ubiquitous, from the magnetic and superconducting transitions in real materials to the cooling of the early universe. Near a second-order transition, a diverging correlation length emerges, and several macroscopic properties become independent of microscopic details of the system [1–3]. Systems can be classified into few universality classes, depending on a small number of global features like symmetry, dimensionality and the range of interactions. Typically, physical quantities exhibit power-law behaviors governed by critical exponents characteristic of a universality class. In particular, at criticality, the two-point correlation function $g(r)$ decays algebraically with the spatial distance r as

$$g(r) \sim r^{2-d-\eta}, \tag{1}$$

where d is the spatial dimension and η is the anomalous dimension. Power-law universality has been extensively verified and recognized as the standard scenario of critical phenomena [2–5]. Very recently, a novel logarithmic universality of criticality, drastically different from that encoded in Eq. (1), was proposed in the context of surface critical behavior (SCB) [6].

SCB refers to the critical phenomenon occurring on the boundary of a critical bulk [6–19]. Recent activities on SCB were partly triggered by the exotic surface effects of symmetry protected topological phases [20,21]. The $\mathrm{O}(N)$ model exhibits rich SCBs including the *special*, *ordinary*, and *extraordinary* transitions, depending on N and d [6–19]. The situations at $d = 3$ are extremely subtle and controversial [6,12,13,18,19]. Logarithmic universality of extraordinary transition was proposed for the three-dimensional $\mathrm{O}(N)$ model with $2 \leq N < N_c$ by means of the renormalization group (RG) [6], whereas N_c is not exactly known. It was predicted that the two-point correlation on the surface decays logarithmically with r as [6]

$$g(r) \sim [\ln(r/r_0)]^{-\hat{\eta}}, \tag{2}$$

where r_0 is a nonuniversal constant. If N is specified, the critical exponent $\hat{\eta}$ is universal in the extraordinary regime. The asymptotic form (2) obviously differs from the standard scenario (1). A quantum Monte Carlo study was performed for the SCB of a $(2+1)$-dimensional O(3) system [18]. However, both the logarithmic and the extraordinary-power behavior [6] were not completely confirmed. By contrast, compelling evidence for the logarithmic behavior was obtained from a classical O(3) ϕ^4 model [19].

In this work, we explore the extraordinary transition with $N = 2$, which is the lower-marginal candidate for the logarithmic universality. We consider an extensive domain of extraordinary critical line, in which the universality of logarithmic behavior is confirmed. Moreover, we give a two-distance scenario for the finite-size scaling (FSS) of $g(r)$, where an r-independent plateau emerges at large distance. The height of the plateau exhibits a logarithmic FSS with the exponent $\hat{\eta}'$, which relates to the exponent $\hat{\eta}$ of r-dependent behavior by $\hat{\eta}' \approx \hat{\eta} - 1$.

Main results.—We study the XY model on simple-cubic lattices with the Hamiltonian [9,12]

$$\mathcal{H}/(k_B T) = -\sum_{\langle \mathbf{r}\mathbf{r}' \rangle} K_{\mathbf{r}\mathbf{r}'} \vec{S}_{\mathbf{r}} \cdot \vec{S}_{\mathbf{r}'}, \tag{3}$$

where $\vec{S}_{\mathbf{r}}$ represents the XY spin on site $\mathbf{r}$ and $K_{\mathbf{r}\mathbf{r}'}$ denotes the strength of the nearest-neighbor ferromagnetic coupling. We impose open boundary conditions in one direction and periodic boundary conditions in other directions, hence a pair of open surfaces are specified. We set $K_{\mathbf{r}\mathbf{r}'} = K'$ if $\mathbf{r}$ and $\mathbf{r}'$ are on the same surface and $K_{\mathbf{r}\mathbf{r}'} = K$ otherwise. The surface coupling enhancement κ is defined by $\kappa = (K' - K)/K$.

Figure 1 shows the phase diagram of model (3), which contains a long-range-ordered surface phase in the presence of ordered bulk, as well as disordered and critical quasi-long-range-ordered surface phases in the presence of disordered bulk. The critical lines meet together at the special transition point. A characteristic feature for $N = 2$ is the existence of the quasi-long-range-ordered phase, which is absent in $N = 1$ and $N \geq 3$ situations.

Consider the quasi-long-range-ordered regime. As the bulk critical point K_c is approached, namely, $K \to K_c^-$, divergent bulk correlations emerge. A possible scenario is that the surface long-range order develops at K_c as a result

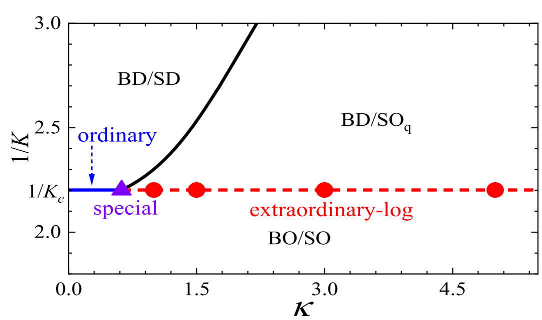

FIG. 1. Phase diagram of the XY model (3). The horizontal axis is for the surface coupling enhancement κ and the vertical axis relates to the bulk coupling K by $1/K$. Phases are denoted by the abbreviations BD (bulk disorder), BO (bulk order), SD (surface disorder), SO_q (surface quasi-long-range order), and SO (surface order). The ordinary, the extraordinary-log, and the SD-SO_q critical lines meet together at the special critical point. The topology of the phase diagram is well known, but the nature of the extraordinary transition remains a puzzle [6]. Parameters denoted by red circles are used in this work to analyze the extraordinary-log universality class.

of the effective interactions mediated by long-range bulk correlations. This scenario cannot be precluded by the Mermin-Wagner theorem as the effective interactions could be long ranged. A previous study revealed [12] that the Monte Carlo data restricting to $L \leq 95$ (L is linear size) are not sufficient to preclude either discontinuous or continuous surface transition across the extraordinary critical line; the former implies long-range surface order at K_c.

By Monte Carlo sampling of the surface two-point correlation function $g(r) = \langle \vec{S}_0 \cdot \vec{S}_r \rangle$, we confirm the emergence of logarithmic universality in model (3). As shown in Fig. 2(a), the L dependence of $g(L/2)$ obeys the scaling formula $g(L/2) \sim [\ln(L/l_0)]^{-\hat{\eta}'}$ with $\hat{\eta}' = 0.59(2)$.

We analyze the surface magnetic fluctuations $\Gamma(\mathbf{k}) = L^2 \langle \| \vec{m}(\mathbf{k}) \|^2 \rangle$ with $\vec{m}(\mathbf{k}) = (1/L^2) \sum_{\mathbf{r}} \vec{S}_{\mathbf{r}} e^{i\mathbf{k}\cdot\mathbf{r}}$, where the summation runs over sites on the surface and $\mathbf{k}$ denotes a Fourier mode. As shown in Figs. 2(a) and 2(b), the magnetic fluctuations $\chi_0 = \Gamma(0,0)$ (susceptibility) and $\chi_1 = \Gamma(2\pi/L, 0)$ have the distinct FSS behaviors $\chi_0 \sim L^2 [\ln(L/l_0)]^{-\hat{\eta}'}$ and $\chi_1 \sim L^2 [\ln(L/l_0)]^{-\hat{\eta}}$, with $\hat{\eta} \approx \hat{\eta}' + 1$. Motivated by these observations as well as the two-distance scenarios in high-dimensional O(N) critical systems [22–26] and quantum deconfined criticality [27], we conjecture that the FSS of critical two-point correlation behaves as

$$g(r) \sim \begin{cases} [\ln(r/r_0)]^{-\hat{\eta}}, & \ln r \leq \mathcal{O}[(\ln L)^{\hat{\eta}'/\hat{\eta}}], \\ [\ln(L/l_0)]^{-\hat{\eta}'}, & \ln r \geq \mathcal{O}[(\ln L)^{\hat{\eta}'/\hat{\eta}}], \end{cases} \tag{4}$$

where r_0 and l_0 are nonuniversal constants. By Eq. (4), we point out two coexisting features: the r-dependent behavior $[\ln(r/r_0)]^{-\hat{\eta}}$ and the large-distance r-independent plateau $[\ln(L/l_0)]^{-\hat{\eta}'}$. Equation (4) is an explanation for our numerical results and compatible with the FSS of second-moment correlation length at the extraordinary transition of the O(3) model [19,28]. Recently, a two-distance scenario was used to describe the two-point correlation of the O(n) model at a marginal situation (the upper critical dimensionality) [25] and confirmed by large-scale simulations on hypercubic lattices up to 768^4 sites [26]. The open surfaces of model (3) are at the lower critical dimensionality ($d_s = 2$) and also belong to marginal situations.

We confirm the scaling relation between $\hat{\eta}'$ and the RG parameter of the helicity modulus. The helicity modulus Υ measures the response of a system to a twist in boundary conditions [29]. The definition is given in the Supplemental Material [30]. Figure 2(c) demonstrates that Υ scales as $\Upsilon L \sim 2\alpha \ln L$ with the RG parameter $\alpha = 0.27(2)$. Figure 3 simultaneously illustrates the universality of $\hat{\eta}'$ and α in the extraordinary regime. Meanwhile, the scaling relation $\alpha \hat{\eta}' = 1/(2\pi)$ is evidenced, conforming to the predicted form [6]

$$\hat{\eta}' = \frac{N-1}{2\pi\alpha}. \tag{5}$$

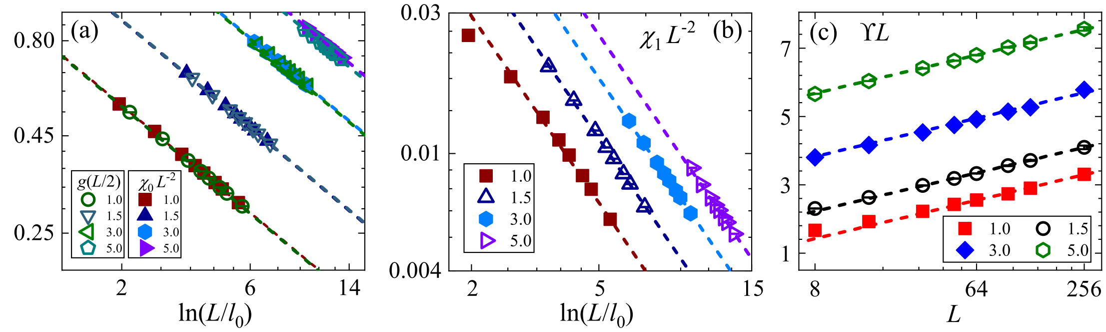

FIG. 2. Results for the extraordinary-log transitions at $\kappa = 1$, 1.5, 3, and 5. Statistical errors are much smaller than the size of symbols. (a) Log-log plot of the two-point correlation $g(L/2)$ and the scaled susceptibility $\chi_0 L^{-2}$ versus $\ln(L/l_0)$. The parameter l_0 is κ dependent and obtained from least-squares fits. Dashed lines have the slope -0.59 and denote the critical exponent $\hat{\eta}' = 0.59(2)$. (b) Log-log plot of the scaled magnetic fluctuations $\chi_1 L^{-2}$ versus $\ln(L/l_0)$. Dashed lines have the slope -1.59 and denote the exponent $\hat{\eta} \approx 1.59$. (c) Scaled helicity modulus ΥL versus L. The horizontal axis is in a log scale. Dashed lines have the slope 0.54 and relate to the universal RG parameter $\alpha = 0.27(2)$ by 2α.

According to Eq. (4), the exponent $\hat{\eta}'$ characterizes the FSS of the height of the plateau. Equation (5) is not exactly the original prediction in Ref. [6], where the exponent $\hat{\eta}$ for r-dependent behavior obeys the relation $\hat{\eta} = (N-1)/(2\pi\alpha)$.

Technique aspects.—To explore the SCB, we fix the bulk coupling strength at K_c. Previously, two of us and co-workers performed simulations utilizing the Prokof'ev-Svistunov worm algorithms [31,32] on periodic simple-cubic lattices with $L_{\max} = 512$, and obtained $1/K_c = 2.2018441(5)$ [33]. This estimate was confirmed by an independent Monte Carlo study [34]. Here, we simulate model (3) at $1/K_c = 2.2018441$ using Wolff's cluster algorithm [35] on simple-cubic lattices with $L_{\max} = 256$. The original procedure in Ref. [35] is adapted to model (3). We analyze the extraordinary transitions at $\kappa = 1$, 1.5, 3, and 5, and the special transition at $\kappa_s = 0.6222$ [12]. For each κ, the number of Wolff updating steps is up to 1.2×10^8 for $L \leq 32$ and ranges from 1.7×10^8 to 6.1×10^8 for $L \geq 48$. See the Supplemental Material [30] for details, which includes Refs. [36,37].

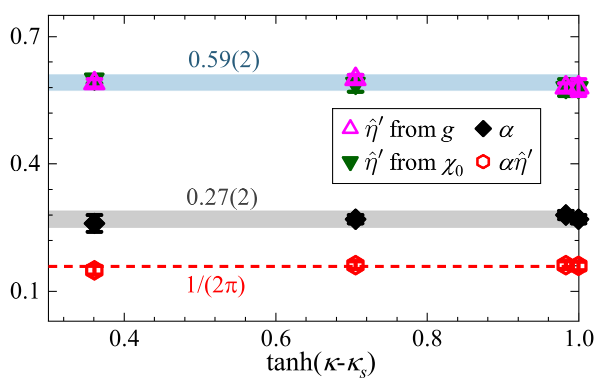

FIG. 3. The critical exponent $\hat{\eta}'$ estimated from $g(L/2)$ and χ_0, the RG parameter α from Υ, and their product $\alpha\hat{\eta}'$. Error bars are plotted with symbols. The shadowed areas, whose heights represent two error bars, denote the ranges of our final estimates for $\hat{\eta}'$ and α. The red dashed line denotes the predicted value $\alpha\hat{\eta}' = 1/(2\pi)$ by RG.

Our conclusions are based on FSS analyses performed by using least-squares fits. Following Refs. [34,38], the function *curve_fit*() in *Scipy_library* is adopted. For caution, we compare the fits with the benchmarks from implementing *Mathematica*'s *NonlinearModelFit* function as Ref. [39]. The fits with the Chi squared per degree of freedom $\chi^2/\mathrm{DOF} \sim 1$ are preferred. We do not trust any single fit and final conclusions are drawn based on comparing the fits that are stable against varying $L_{\min}$, the minimum size incorporated.

Emergence of logarithmic universality.—Figure 4(a) demonstrates the two-point correlation function $g(r)$ for the extraordinary transition at $\kappa = 1$. The large-distance behavior can be monitored by the L dependence of $g(L/2)$. According to Eq. (4), we have a scaling formula $g(L/2) \sim [\ln(L/l_0)]^{-\hat{\eta}'}$. We perform least-squares fits to this formula and obtain $\hat{\eta}' = 0.596(2)$, $l_0 = 0.94(1)$, and $\chi^2/\mathrm{DOF} \approx 0.73$, with $L_{\min} = 16$. As $L_{\min}$ is varied, preferred fits are also obtained (Table I). By comparing the fits, our final estimate of $\hat{\eta}'$ for $\kappa = 1$ is $\hat{\eta}' = 0.59(1)$. In the Supplemental Material [30], we present similar analyses for $\kappa = 1.5$, 3, and 5, for which the final estimates are $\hat{\eta}' = 0.60(1)$ ($\kappa = 1.5$), 0.58(1) ($\kappa = 3$), and 0.58(2) ($\kappa = 5$). It is therefore confirmed that $g(L/2)$ obeys the logarithmic scaling $g(L/2) \sim [\ln(L/l_0)]^{-\hat{\eta}'}$, with a universal exponent $\hat{\eta}' = 0.59(2)$. As displayed in the Supplemental Material [30], the fits by the conventional power-law ansatz (1) have poor qualities and give unstable results.

Existence of two distinct exponents.—For a verification of Eq. (4), we analyze the FSS of surface magnetic fluctuations. In the Monte Carlo simulations, we sample $\chi_2 = \Gamma(2\pi/L, 2\pi/L)$ as well as χ_0 and χ_1.

According to Eq. (4), an r-independent plateau emerges at large distance. This plateau contributes to the magnetic fluctuations at zero mode but not to those at nonzero

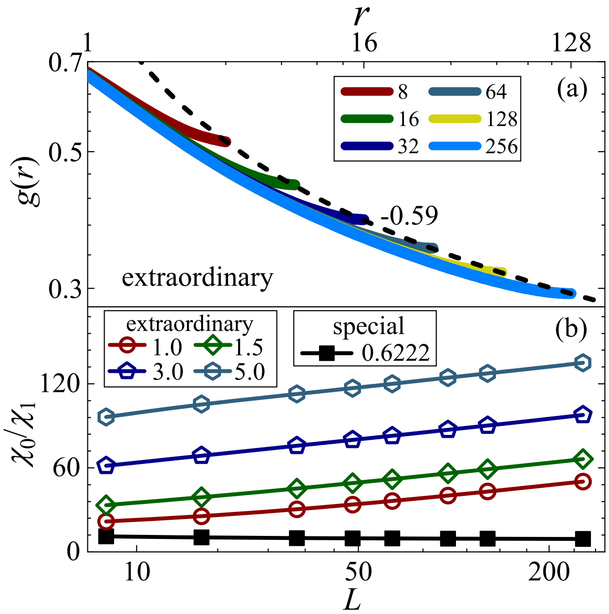

FIG. 4. (a) The two-point correlation $g(r)$ for the extraordinary-log transition at $\kappa = 1$ with $L = 8$, 16, 32, 64, 128, and 256. The dashed line denotes the logarithmic decaying $[\ln(L/l_0)]^{-0.59}$ in the large-distance limit. (b) The ratio χ_0/χ_1 of magnetic fluctuations versus L for the extraordinary-log transitions at $\kappa = 1$, 1.5, 3, and 5, and for the special transition at $\kappa_s = 0.6222$. In both panels, statistical errors are much smaller than the sizes of the data points.

modes. The ratio χ_0/χ_1 at extraordinary transitions is shown in Fig. 4(b). As $L \to \infty$, the ratio keeps increasing, implying distinct FSS of χ_0 and χ_1.

More precisely, χ_0 is expected to scale as $\chi_0 \sim L^2[\ln(L/l_0)]^{-\hat{\eta}'}$. The results of scaling analyses for $\kappa = 1$ are illustrated in Table I and those for $\kappa = 1.5$, 3, and 5 are given in the Supplemental Material [30]. Comparing preferred fits, we obtain $\hat{\eta}' = 0.60(1)$ ($\kappa = 1$), 0.59(2) ($\kappa = 1.5$), 0.58(2) ($\kappa = 3$), and 0.58(1) ($\kappa = 5$). These estimates of $\hat{\eta}'$ agree well with those determined from the L dependence of $g(L/2)$, hence the final result $\hat{\eta}' = 0.59(2)$ is confirmed.

TABLE I. Estimates of the critical exponent $\hat{\eta}'$ and the RG parameter α for the extraordinary-log transition at $\kappa = 1$. $\hat{\eta}'$ is estimated from the scaling formulas $g(L/2) \sim [\ln(L/l_0)]^{-\hat{\eta}'}$ and $\chi_0 \sim L^2[\ln(L/l_0)]^{-\hat{\eta}'}$, and α is determined from $\Upsilon L = 2\alpha \ln L + A + BL^{-1}$.

	$L_{\min}$	χ^2/DOF	$\hat{\eta}'$ or α	l_0 or A
$g(L/2)$	16	2.91/4	0.596(2)	0.94(1)
	32	0.66/3	0.592(3)	0.97(2)
	48	0.58/2	0.591(5)	0.98(4)
χ_0	32	3.46/3	0.603(2)	1.13(2)
	48	0.08/2	0.598(4)	1.18(3)
	64	0.02/1	0.597(5)	1.19(5)
Υ	8	5.46/4	0.255(3)	0.41(2)
	16	3.33/3	0.265(7)	0.32(6)
	32	2.51/2	0.25(2)	0.4(2)

We analyze the magnetic fluctuations χ_1 and χ_2 at nonzero Fourier modes by performing fits to $\chi_{\mathbf{k}\neq 0} \sim L^2[\ln(L/l_0)]^{-\hat{\eta}}$. We confirm the drastic decays of $\chi_1 L^{-2}$ and $\chi_2 L^{-2}$ upon increasing $\ln L$. For reducing the uncertainties of fits, we fix l_0 at those obtained from the scaling analyses of χ_0, and estimate $\hat{\eta} \approx 1.7$ over $\kappa = 1$, 1.5, 3, and 5. From the log-log plot of $\chi_1 L^{-2}$ versus $\ln(L/l_0)$ in Fig. 2(b), it is seen that the data nearly scale as $\chi_1 L^{-2} \sim [\ln(L/l_0)]^{-\hat{\eta}}$ with $\hat{\eta} \approx 1.59$. A similar result is obtained for $\chi_2 L^{-2}$ (Supplemental Material [30]). Hence, χ_1 and χ_2 obey the logarithmic FSS formula $\chi_{\mathbf{k}\neq 0} \sim L^2[\ln(L/l_0)]^{-\hat{\eta}}$, with $\hat{\eta} \approx 1.6$.

Our results for the FSS of χ_0 and χ_1 are also compatible with the Monte Carlo data [19,28] of the second-moment correlation length ξ_{2nd}, which scales as $(\xi_{\text{2nd}}/L)^2 \sim (\chi_0/\chi_1 - 1) \sim \ln L$. The relation $\hat{\eta} = \hat{\eta}' + 1$ is implied.

As $\hat{\eta}$ is much larger than $\hat{\eta}'$, the two-distance scenario (4) indicates that the r-dependent contribution decays fast. It explains the profile of $g(r)$ in Fig. 4(a), where the large-distance plateau dominates.

By contrast, the special transition at κ_s belongs to the standard scenario (1) of continuous transition. The r-dependent behavior converges to the power law $g(r) \sim r^{-\eta}$, which is comparable with the contribution from $g(L/2) \sim L^{-\eta}$. Moreover, the magnetic renormalization exponent y_h relates to the anomalous dimension η by $y_h = (4 - \eta)/2$, and the magnetic fluctuations χ_0, χ_1, and χ_2 *all* scale as $L^{2y_h - 2}$. As shown in Fig. 4(b), the ratio χ_0/χ_1 at κ_s converges fast to a constant upon increasing L. More results for $g(r)$, χ_0, χ_1, and χ_2 are given in the Supplemental Material [30].

Scaling relation.—It was predicted [6,28] that the scaled helicity modulus ΥL diverges logarithmically as $\Upsilon L \sim 2\alpha \ln L$, with α a universal RG parameter. Further, the universal form (5) of scaling relation was established [6]. The form is supported by the Monte Carlo results of an O(3) ϕ^4 model [19].

We sample Υ of model (3) by Monte Carlo simulations. The dependence of ΥL on $\ln L$ is shown in Fig. 2(c) for $\kappa = 1$, 1.5, 3, and 5. For each κ, a nearly linear dependence is observed in large-L regime. Further, we perform a FSS analysis of Υ according to $\Upsilon L = 2\alpha \ln L + A + BL^{-1}$, where A and B are constants. We explore the situations with and without the correction term BL^{-1} separately. Stable fits are achieved, with the final estimates of α being $\alpha = 0.26(2)$ ($\kappa = 1$), 0.27(1) ($\kappa = 1.5$), 0.28(1) ($\kappa = 3$), and 0.27(1) ($\kappa = 5$). Comparing these estimates, the universal value of α is determined to be $\alpha = 0.27(2)$.

As shown in Fig. 3, the scaling relation (5) between α and $\hat{\eta}'$ is confirmed. According to Eq. (4), $\hat{\eta}'$ characterizes the logarithmic FSS for the height of the plateau.

Discussions.—We provide strong evidence for the emergence of the extraordinary-log universality class [6]. We propose the two-distance scenario (4) for the FSS of the two-point correlation function, where a large-distance plateau emerges. The height of the plateau decays logarithmically with L by the exponent $\hat{\eta}'$, which obeys the scaling relation (5) with the RG parameter of helicity modulus. The two-distance scenario is supported not only by the Monte Carlo data for $N = 2$ of this work, but also by the results for $N = 3$ in Ref. [19].

A variety of open questions arise. First, it is shown essentially that a two-dimensional XY system with *finely tuned* long-range interactions exhibits logarithmic universality. Is it possible to formulate the interactions in a microscopic Hamiltonian? Second, is there a classical-quantum mapping for the two-distance scenario that holds at the O(N) quantum critical points [16–18]? Third, as shown in Ref. [26], the introduction of unwrapped distance is crucial for verifying the short-distance behavior in two-distance scenario. The behavior of unwrapped distance in the extraordinary-log universality remains unclear. Finally, we note that, as recently observed for the five-dimensional Ising model [40], lattice sites can be decomposed into clusters, and interesting geometric phenomena associated with the two-distance scenario may arise [41].

We thank Max Metlitski for useful comments and for sharing an unpublished note [28] with us. This work has been supported by the National Natural Science Foundation of China (under Grants No. 11774002, No. 11625522, and No. 11975024), the Science and Technology Committee of Shanghai (under Grant No. 20DZ2210100), the National Key R&D Program of China (under Grant No. 2018YFA0306501), and the Education Department of Anhui.

[*]yjdeng@ustc.edu.cn
[†]jplv2014@ahnu.edu.cn

[1] H. E. Stanley, Scaling, universality, and renormalization: Three pillars of modern critical phenomena, Rev. Mod. Phys. **71**, S358 (1999).
[2] S. Sachdev, *Quantum Phase Transitions* (Cambridge University Press, Cambridge, England, 2011).
[3] R. Fernández, J. Fröhlich, and A. D. Sokal, *Random Walks, Critical Phenomena, and Triviality in Quantum Field Theory* (Springer, Berlin, 2013).
[4] A. Goldman, *Percolation, Localization, and Superconductivity* (Springer, Boston, 2013), Vol. 109.
[5] B. V. Svistunov, E. S. Babaev, and N. V. Prokof'ev, *Superfluid States of Matter* (CRC Press, London, 2015).
[6] M. A. Metlitski, Boundary criticality of the $o(n)$ model in $d = 3$ critically revisited, arXiv:2009.05119.
[7] K Binder and P. C. Hohenberg, Surface effects on magnetic phase transitions, Phys. Rev. B **9**, 2194 (1974).
[8] K. Ohno and Y. Okabe, The 1/n expansion for the extraordinary transition of semi-infinite system, Prog. Theor. Phys. **72**, 736 (1984).
[9] D. P. Landau, R. Pandey, and K. Binder, Monte Carlo study of surface critical behavior in the xy model, Phys. Rev. B **39**, 12302 (1989).
[10] H. W. Diehl, The theory of boundary critical phenomena, Int. J. Mod. Phys. B **11**, 3503 (1997).
[11] M. Pleimling, Critical phenomena at perfect and non-perfect surfaces, J. Phys. A **37**, R79 (2004).
[12] Y. Deng, H. W. J. Blöte, and M. P. Nightingale, Surface and bulk transitions in three-dimensional $o(n)$ models, Phys. Rev. E **72**, 016128 (2005).
[13] Y. Deng, Bulk and surface phase transitions in the three-dimensional $o(4)$ spin model, Phys. Rev. E **73**, 056116 (2006).
[14] J. Dubail, J. L. Jacobsen, and H. Saleur, Exact Solution of the Anisotropic Special Transition in the $o(n)$ Model in Two Dimensions, Phys. Rev. Lett. **103**, 145701 (2009).
[15] L. Zhang and F. Wang, Unconventional Surface Critical Behavior Induced by a Quantum Phase Transition from the Two-Dimensional Affleck-Kennedy-Lieb-Tasaki Phase to a Néel-Ordered Phase, Phys. Rev. Lett. **118**, 087201 (2017).
[16] C. Ding, L. Zhang, and W. Guo, Engineering Surface Critical Behavior of $(2+1)$-Dimensional $o(3)$ Quantum Critical Points, Phys. Rev. Lett. **120**, 235701 (2018).
[17] L. Weber, F. Parisen Toldin, and S. Wessel, Nonordinary edge criticality of two-dimensional quantum critical magnets, Phys. Rev. B **98**, 140403(R) (2018).
[18] L. Weber and S. Wessel, Spin versus bond correlations along dangling edges of quantum critical magnets, Phys. Rev. B **103**, L020406 (2021).
[19] F. Parisen Toldin, Boundary Critical Behavior of the Three-Dimensional Heisenberg Universality Class, Phys. Rev. Lett. **126**, 135701 (2021).
[20] T. Grover and A. Vishwanath, Quantum criticality in topological insulators and superconductors: Emergence of strongly coupled majoranas and supersymmetry, arXiv: 1206.1332.
[21] D. E. Parker, T. Scaffidi, and R. Vasseur, Topological Luttinger liquids from decorated domain walls, Phys. Rev. B **97**, 165114 (2018).
[22] V. Papathanakos, Ph.D. thesis, Princeton University, Princeton, New Jersey, 2006.
[23] J. Grimm, E. M. Elçi, Z. Zhou, T. M. Garoni, and Y. Deng, Geometric Explanation of Anomalous Finite-Size Scaling in High Dimensions, Phys. Rev. Lett. **118**, 115701 (2017).
[24] Z. Zhou, J. Grimm, S. Fang, Y. Deng, and T. M. Garoni, Random-Length Random Walks and Finite-Size Scaling in High Dimensions, Phys. Rev. Lett. **121**, 185701 (2018).
[25] J.-P. Lv, W. Xu, Y. Sun, K. Chen, and Y. Deng, Finite-size scaling of $o(n)$ systems at the upper critical dimensionality, Natl. Sci. Rev. **8**, nwaa212 (2021).
[26] S. Fang, Y. Deng, and Z. Zhou, Logarithmic finite-size scaling of the self-avoiding walk at four dimensions, arXiv:2103.04340.
[27] H. Shao, W. Guo, and A. W. Sandvik, Quantum criticality with two length scales, Science **352**, 213 (2016).
[28] M. A. Metlitski, Finite size corrections in the extra-ordinary log phase (private communication).

[29] M. E. Fisher, M. N. Barber, and D. Jasnow, Helicity modulus, superfluidity, and scaling in isotropic systems, Phys. Rev. A **8**, 1111 (1973).

[30] See Supplemental Material at http://link.aps.org/supplemental/10.1103/PhysRevLett.127.120603 for more details.

[31] N. V. Prokof'ev and B. V. Svistunov, Worm Algorithms for Classical Statistical Models, Phys. Rev. Lett. **87**, 160601 (2001).

[32] N. V. Prokof'ev and B. V. Svistunov, Worm algorithm for problems of quantum and classical statistics, in *Understanding Quantum Phase Transitions* (Taylor & Francis, Boca Raton, 2010), pp. 499–522.

[33] W. Xu, Y. Sun, J.-P. Lv, and Y. Deng, High-precision Monte Carlo study of several models in the three-dimensional u(1) universality class, Phys. Rev. B **100**, 064525 (2019).

[34] M. Hasenbusch, Monte Carlo study of an improved clock model in three dimensions, Phys. Rev. B **100**, 224517 (2019).

[35] U. Wolff, Collective Monte Carlo Updating for Spin Systems, Phys. Rev. Lett. **62**, 361 (1989).

[36] W. Janke, Test of single cluster update for the three-dimensional xy model, Phys. Lett. A **148**, 306 (1990).

[37] W. Krauth, *Statistical Mechanics: Algorithms and Computations* (Oxford University Press, New York, 2006).

[38] M. Hasenbusch, Monte Carlo study of a generalized icosahedral model on the simple cubic lattice, Phys. Rev. B **102**, 024406 (2020).

[39] J. Salas, Phase diagram for the bisected-hexagonal-lattice five-state Potts antiferromagnet, Phys. Rev. E **102**, 032124 (2020).

[40] S. Fang, J. Grimm, Z. Zhou, and Y. Deng, Complete graph and Gaussian fixed-point asymptotics in the five-dimensional Fortuin-Kasteleyn Ising model with periodic boundaries, Phys. Rev. E **102**, 022125 (2020).

[41] Y. Sun, M. Hu, Y. Deng, and J.-P. Lv (to be published).